Switching Site-Selectivity with Light in the Acetylation of Sugars with Azo-Peptide Catalysts

07th December 2018

Group Seminar #441

Dominik Niedek

Institute of Organic Chemistry
Justus-Liebig-University
35392 Giessen, Germany

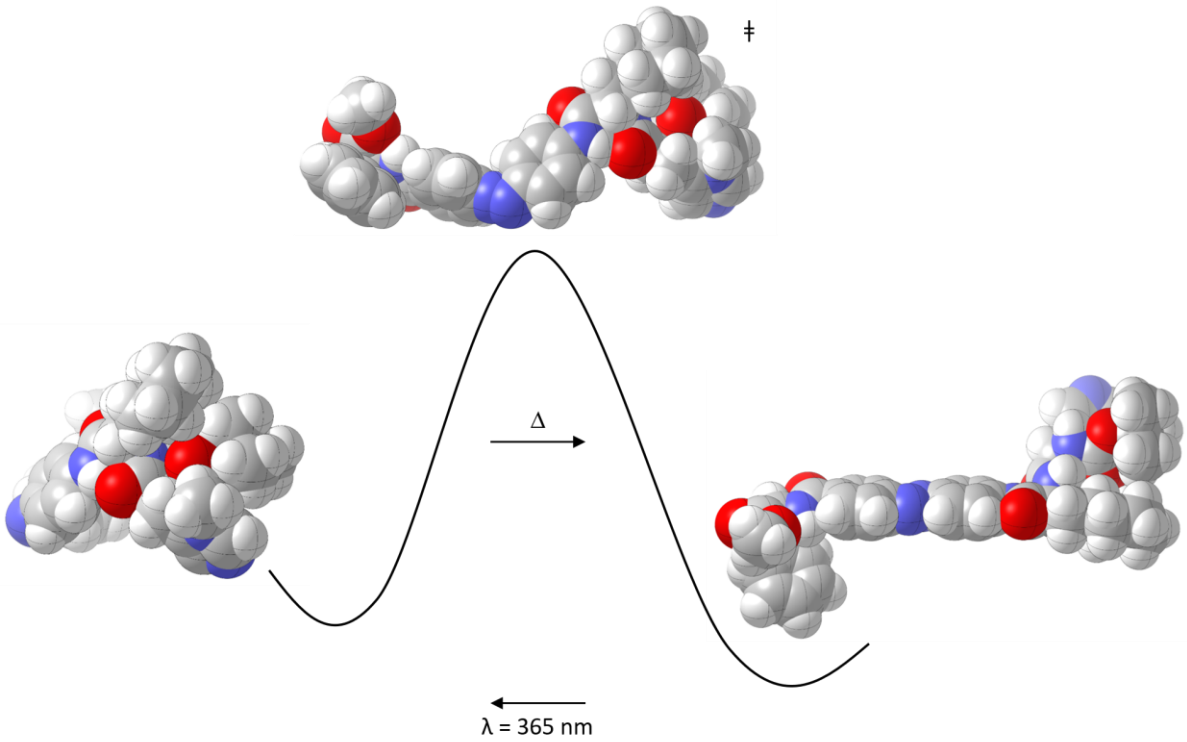

Motivation

"Beyond activity control: Throughout this review we have focused on catalytic activity, encoding the ability of the catalyst to enable and speed up an otherwise unfeasible chemical reaction. However, one of the inherent challenges in catalyst research is not only the mere enabling of a given chemical transformation but also the complete control over its outcome by developing suitable catalysts to dictate chemoselectivity, regioselectivity, and stereoselectivity of the reaction."

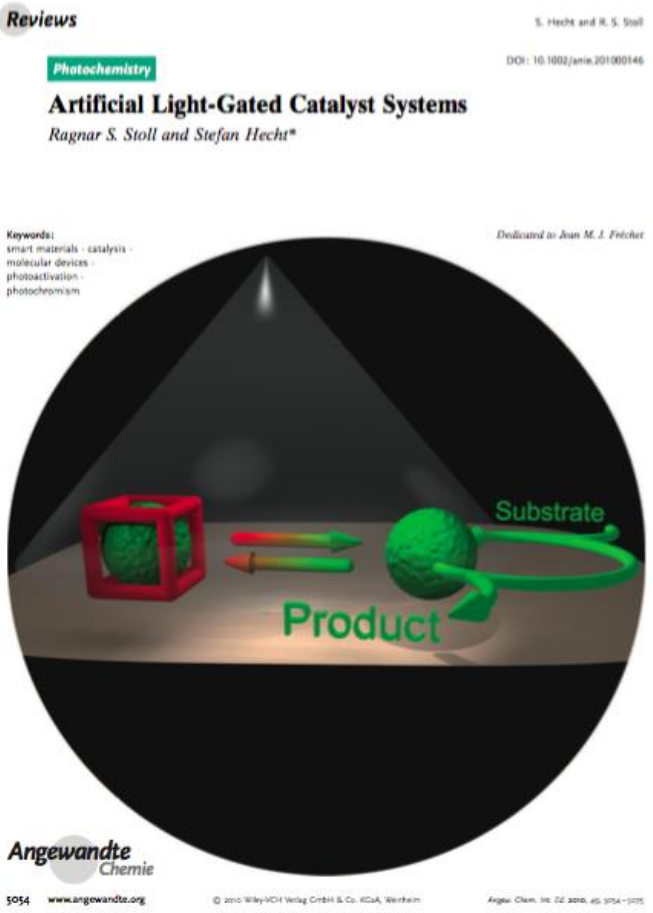

R. S. Stoll, S. Hecht, *Angew. Chem. Int. Ed.* **2010**, *49*, 5054-5075.

Motivation

"Ultimately, photoswitchable catalysis will require the ability to photochemically alter the selectivity of the catalyst in addition to its activity. A system in which the catalyst's intrinsic chemo-, regio-, and/or stereoselectivity could be remotely photomodulated will have numerous applications in tandem catalysis, and is expected to provide unprecedented control over polymer microstructure, as well as to simplify multistep syntheses of complex small molecules."

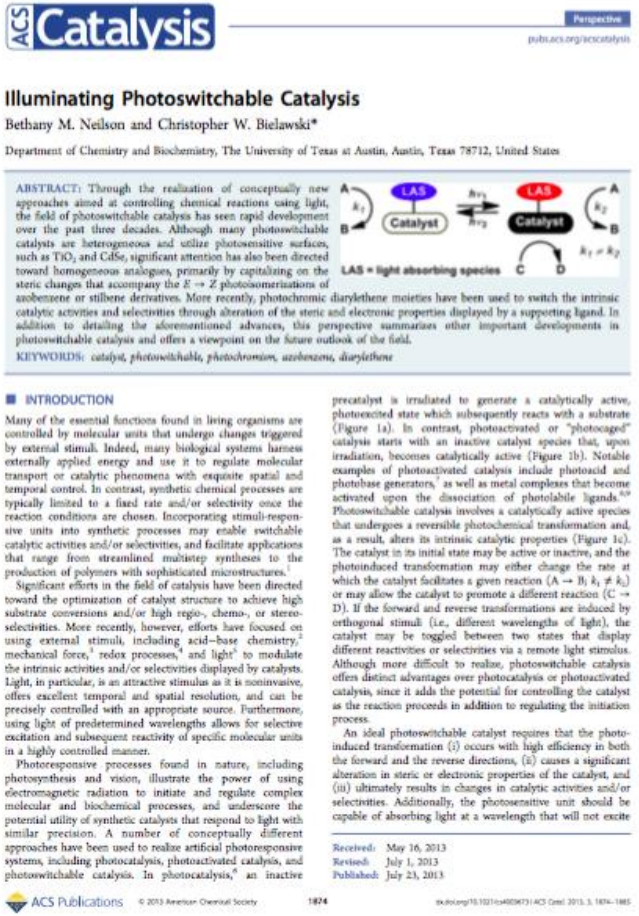

ACS Catalysis

Perspective

pubs.acs.org/acscatalysis

Illuminating Photoswitchable Catalysis

Bethany M. Neilson and Christopher W. Bielawski*

Department of Chemistry and Biochemistry, The University of Texas at Austin, Austin, Texas 78712, United States

ABSTRACT: Through the realization of conceptually new approaches aimed at controlling chemical reactions using light, the field of photoswitchable catalysis has seen rapid development over the past three decades. Although many photoswitchable catalysts are heterogeneous and utilize photosensitive surfaces, such as TiO_2 and CdSe, significant attention has also been directed toward homogeneous analogues, primarily by capitalizing on the steric changes that accompany the $E \rightarrow Z$ photoisomerizations of azobenzene or stilbene derivatives. More recently, photochromic diarylethene moieties have been used to switch the intrinsic catalytic activities and selectivities through alteration of the steric and electronic properties displayed by a supporting ligand. In addition to detailing the aforementioned advances, this perspective summarizes other important developments in photoswitchable catalysis and offers a viewpoint on the future outlook of the field.

KEYWORDS: *catalyst, photoswitchable, photochromism, azobenzene, diarylethene*

INTRODUCTION

Many of the essential functions found in living organisms are controlled by molecular units that undergo changes triggered by external stimuli. Indeed, many biological systems harness externally applied energy and use it to regulate molecular transport or catalytic phenomena with exquisite spatial and temporal control. In contrast, synthetic chemical processes are typically limited to a fixed rate and/or selectivity once the reaction conditions are chosen. Incorporating stimuli-responsive units into synthetic processes may enable switchable catalytic activities and/or selectivities, and facilitate applications that range from streamlined multistep syntheses to the production of polymers with sophisticated microstructures.[1]

Significant efforts in the field of catalysis have been directed toward the optimization of catalyst structure to achieve high substrate conversions and/or high regio-, chemo-, or stereoselectivities. More recently, however, efforts have focused on using external stimuli, including acid−base chemistry,[2] mechanical force,[3] redox processes,[4] and light[5] to modulate the intrinsic activities and/or selectivities displayed by catalysts. Light, in particular, is an attractive stimulus as it is noninvasive, offers excellent temporal and spatial resolution, and can be precisely controlled with an appropriate source. Furthermore, using light of predetermined wavelengths allows for selective excitation and subsequent reactivity of specific molecular units in a highly controlled manner.

Photoresponsive processes found in nature, including photosynthesis and vision, illustrate the power of using electromagnetic radiation to initiate and regulate complex molecular and biochemical processes, and underscore the potential utility of synthetic catalysts that respond to light with similar precision. A number of conceptually different approaches have been used to realize artificial photoresponsive systems, including photocatalysis, photoactivated catalysis, and photoswitchable catalysis. In photocatalysis,[6] an inactive precatalyst is irradiated to generate a catalytically active, photoexcited state which subsequently reacts with a substrate (Figure 1a). In contrast, photoactivated or "photocaged" catalysis starts with an inactive catalyst species that, upon irradiation, becomes catalytically active (Figure 1b). Notable examples of photoactivated catalysis include photoacid and photobase generators,[7] as well as metal complexes that become activated upon the dissociation of photolabile ligands.[8,9] Photoswitchable catalysis involves a catalytically active species that undergoes a reversible photochemical transformation and, as a result, alters its intrinsic catalytic properties (Figure 1c). The catalyst in its initial state may be active or inactive, and the photoinduced transformation may either change the rate at which the catalyst facilitates a given reaction ($A \rightarrow B$; $k_1 \neq k_2$) or may allow the catalyst to promote a different reaction ($C \rightarrow D$). If the forward and reverse transformations are induced by orthogonal stimuli (i.e., different wavelengths of light), the catalyst may be toggled between two states that display different reactivities or selectivities via a remote light stimulus. Although more difficult to realize, photoswitchable catalysis offers distinct advantages over photocatalysis or photoactivated catalysis, since it adds the potential for controlling the catalyst as the reaction proceeds in addition to regulating the initiation process.

An ideal photoswitchable catalyst requires that the photoinduced transformation (i) occurs with high efficiency in both the forward and the reverse directions, (ii) causes a significant alteration in steric or electronic properties of the catalyst, and (iii) ultimately results in changes in catalytic activities and/or selectivities. Additionally, the photosensitive unit should be capable of absorbing light at a wavelength that will not excite

Received: May 16, 2013
Revised: July 1, 2013
Published: July 23, 2013

B. M. Neilson, C. W. Bielawski, *ACS Catalysis* **2013**, *3*, 1874-1885.

Motivation

Even though progress in this field has been remarkable, major barriers remain that need to be overcome. For example, a photoswitchable catalyst capable of catalyzing two orthogonal reactions is yet to be reported. Unlike redox-switchable and ion-switchable systems, in which chemical waste is generated, photoswitchable systems offer major advantages, as they use a clean and noninvasive external trigger that allows spatiotemporal precision.

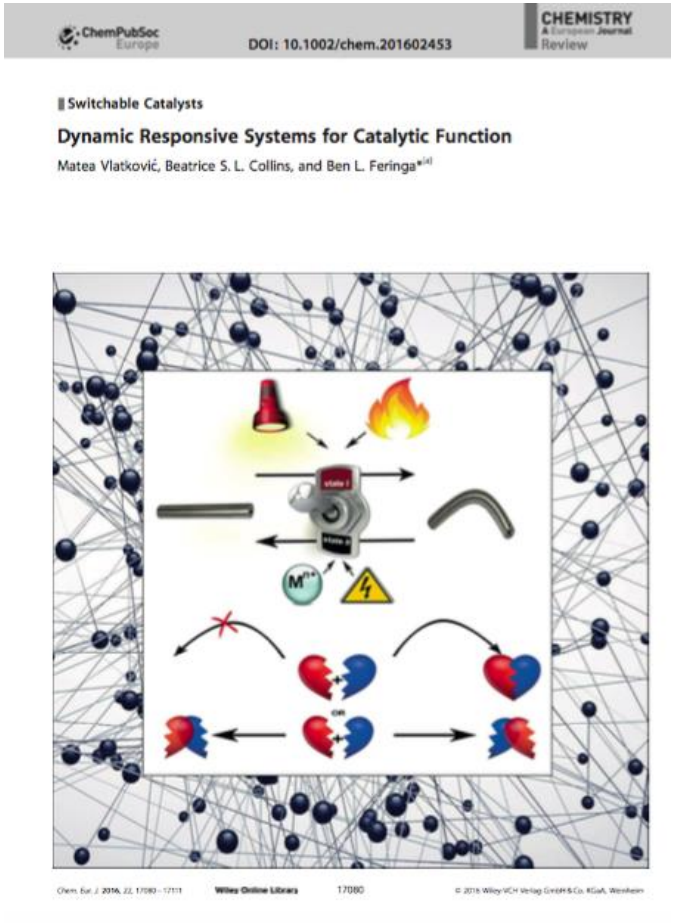

M. Vlatković, B. S. L. Collins, B. L. Feringa, *Chem. Eur. J.* **2016**, *22*, 17080-17111.

Società Chimica Italiana

IUPAC

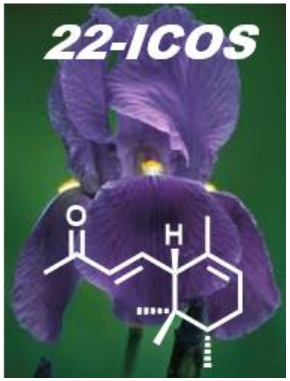

Session 2 - AUDITORIUM – Chair: ANNE NIJS

17:45 – PL2 (60') **B. L. Feringa** - University of Groningen, The Netherlands
Dynamic Molecular Systems

http://www.22-icos-florence.it/conference-program/

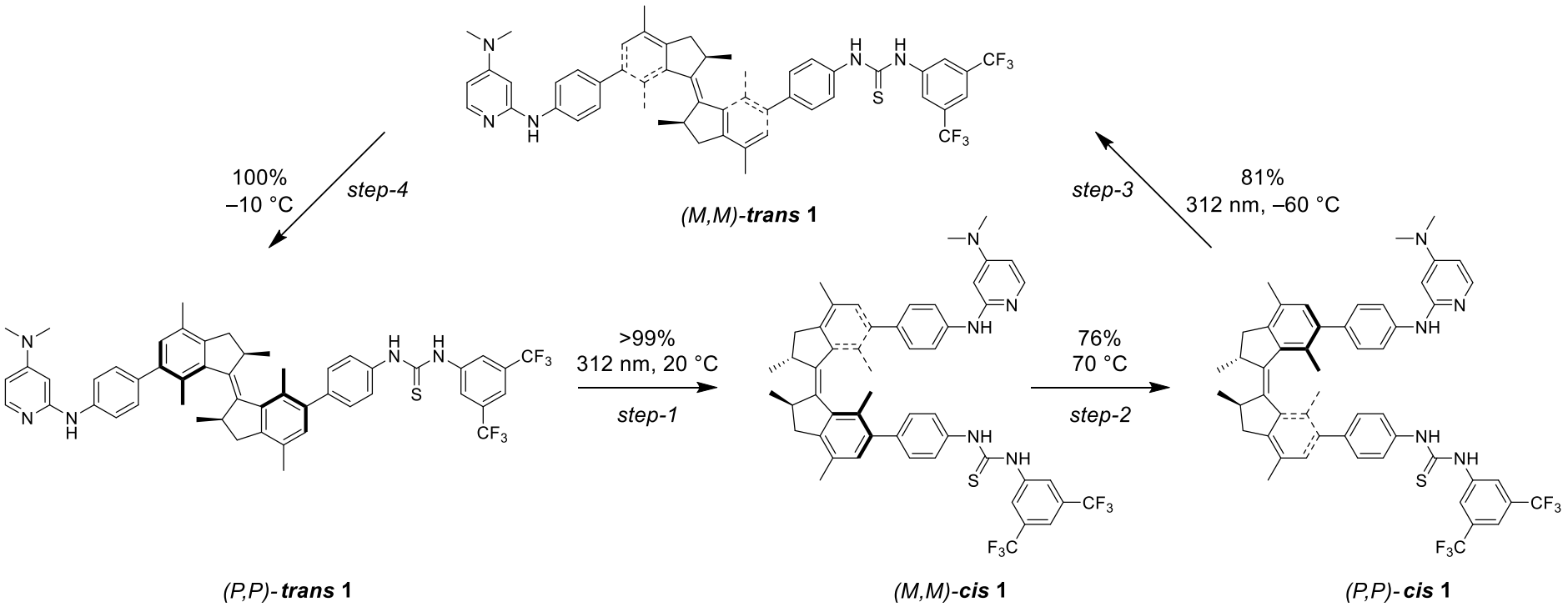

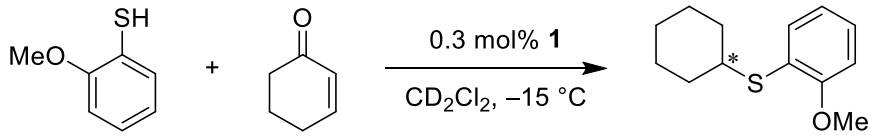

(*P*,*P*)-***trans* 1**: rac.
(*M*,*M*)-***cis* 1**: (***S***) 48% *ee*
(*P*,*P*)-***cis* 1**: (***R***) 50% *ee*

J. Wang, B. L. Feringa, *Science* **2011**, *331*, 1429-1432.

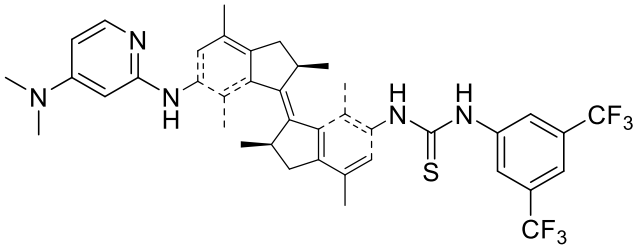

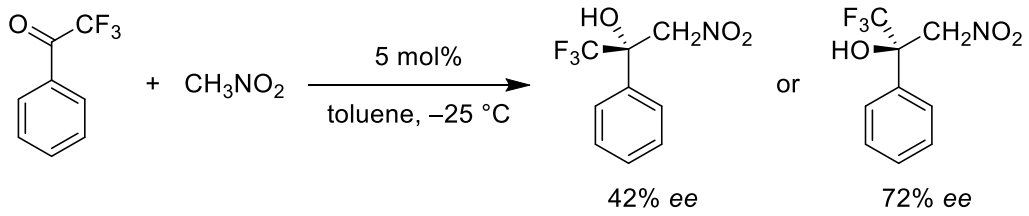

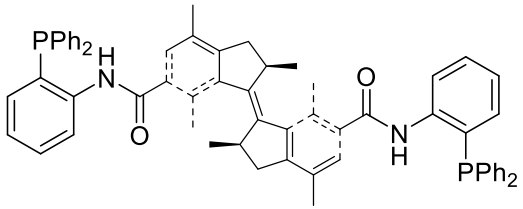

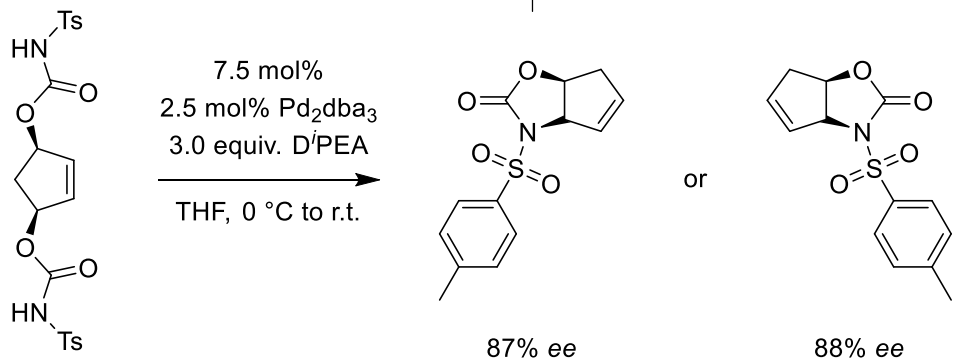

J. Wang, B. L. Feringa, *Science* **2011**, *331*, 1429-1432.

Previous work

1) A–B–C ⟵ (catalyst, //) A–B + C ⟶ (catalyst, external stimulus) A–B–C

2) (***S***)-A–B–C ⟵ (catalyst, external stimulus) A–B + C ⟶ (catalyst, external stimulus) (***R***)-A–B–C

ON/OFF

Switching
Stereoselectivity

This work

3) **C**–A–B ⟵ (catalyst, dark) A–B + **C** ⟶ (catalyst, hv) A–B–**C**

Switching
Site-Selectivity

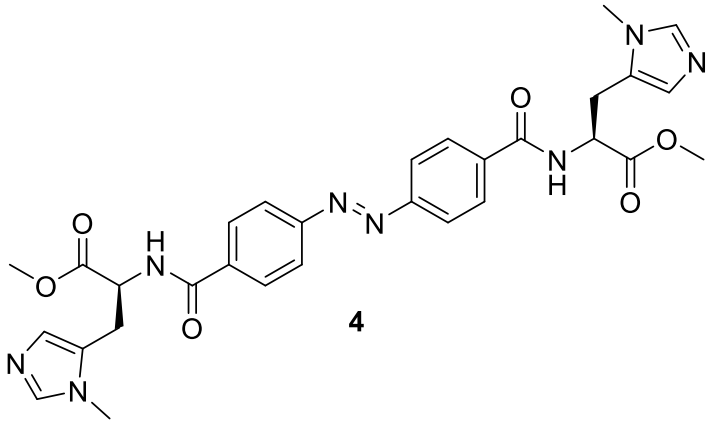

4

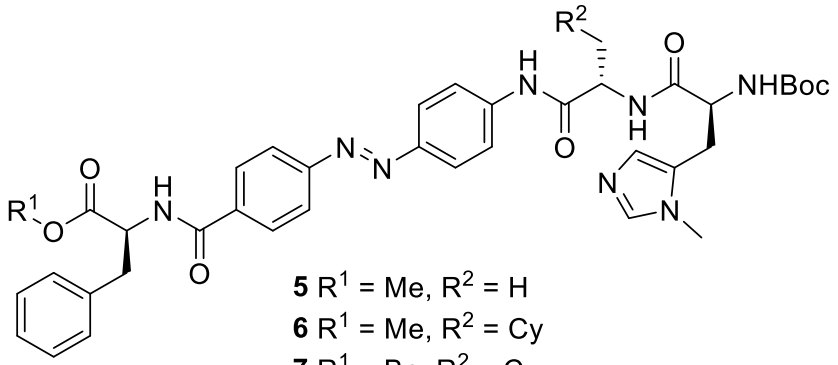

5 R^1 = Me, R^2 = H
6 R^1 = Me, R^2 = Cy
7 R^1 = Bn, R^2 = Cy

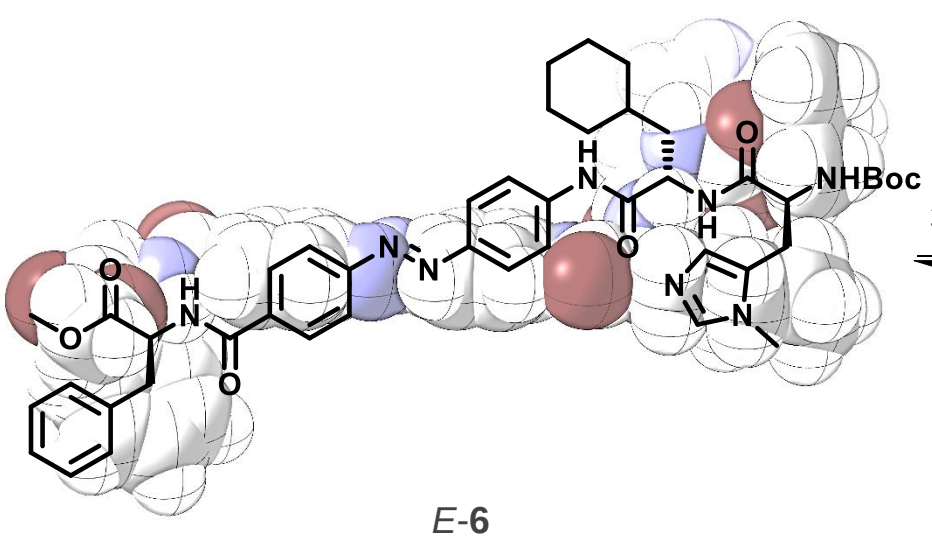

E-**6**

365 nm

Δ

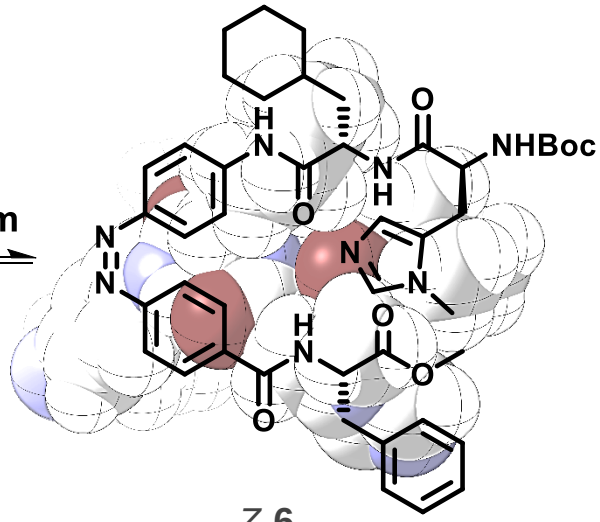

Z-**6**

ΔH_0 = 0.0 (0.0) kcal mol^{-1}

ΔH_0 = 12.4 (10.5) kcal mol^{-1}

B3LYP-D3(BJ)/6-311G(d,p) and DLPNO-CCSD(T)/def2-tzvpp//B3LYP-D3(BJ)/6-311G(d,p) (in parentheses) levels of theory.

Concept to Control Regioselectivity in Acylation Reactions

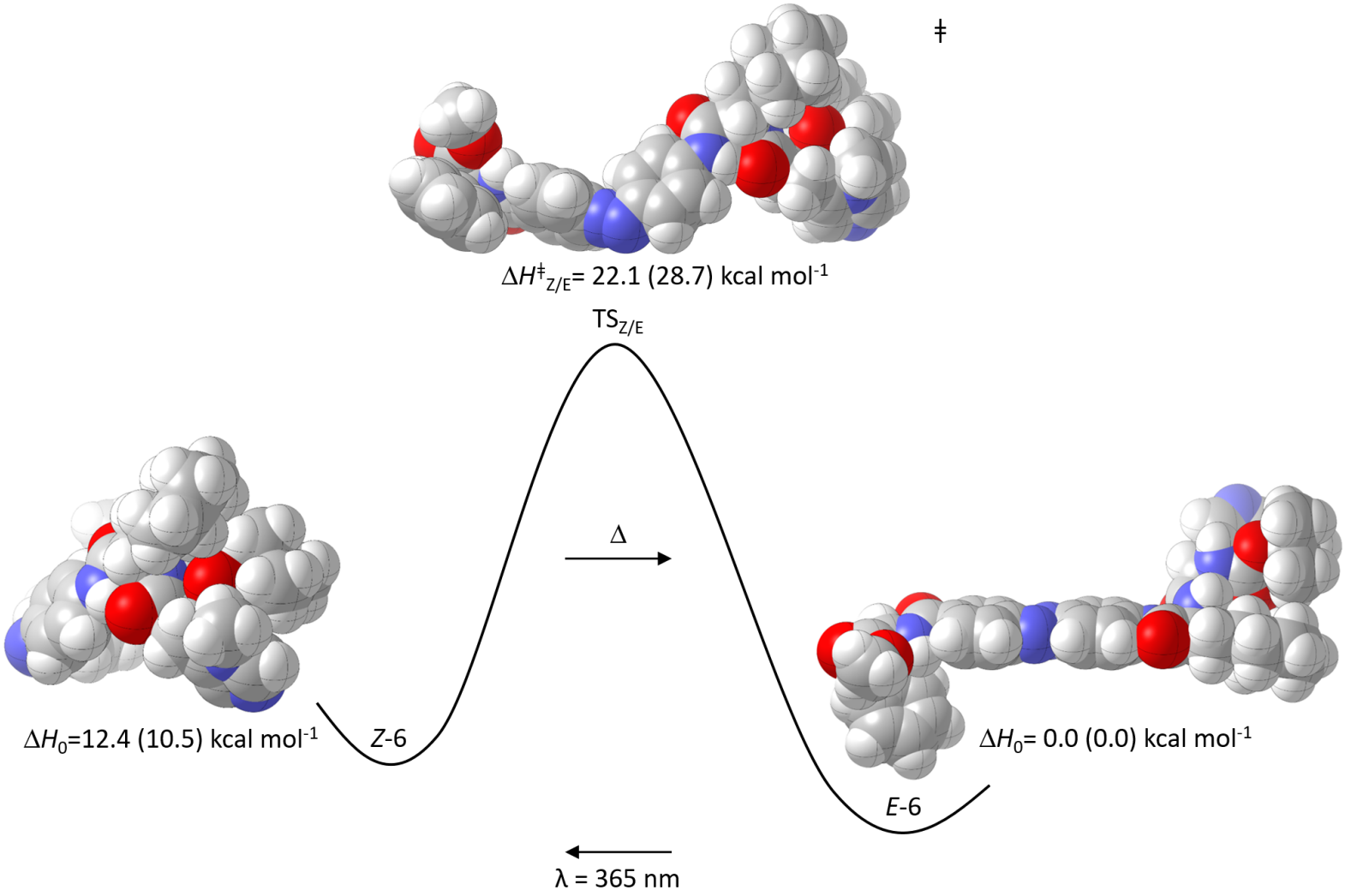

B3LYP-D3(BJ)/6-311G(d,p) and DLPNO-CCSD(T)/def2-tzvpp//B3LYP-D3(BJ)/6-311G(d,p) (in parentheses) levels of theory.

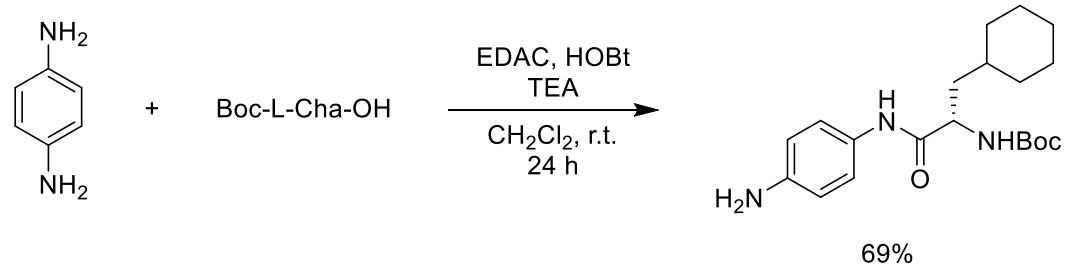
NH2
NH2
+
Boc-L-Cha-OH
EDAC, HOBt
TEA
CH2Cl2, r.t.
24 h
H
N
NHBoc
O
H2N
69%

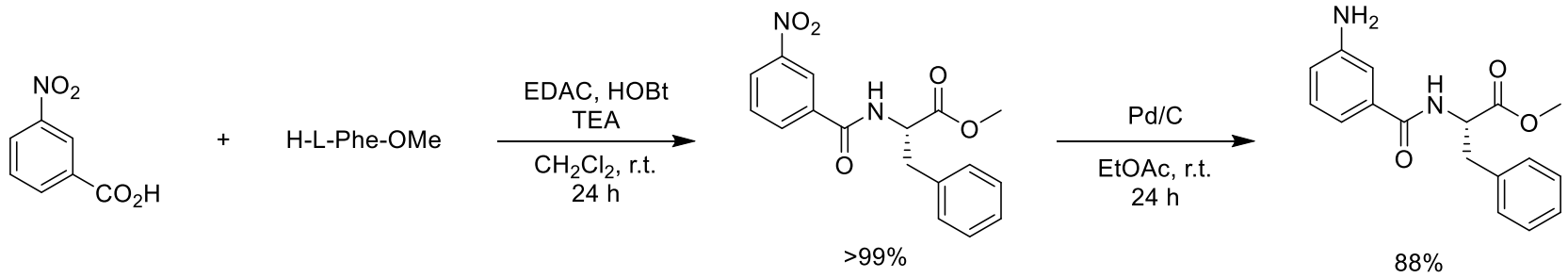
NO2
CO2H
+
H-L-Phe-OMe
EDAC, HOBt
TEA
CH2Cl2, r.t.
24 h
NO2
H
N
O
O
O
>99%
Pd/C
EtOAc, r.t.
24 h
NH2
H
N
O
O
O
88%

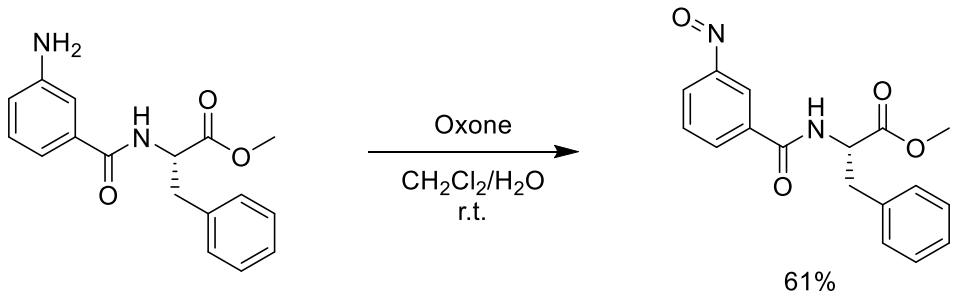
NH2
H
N
O
O
O
Oxone
CH2Cl2/H2O
r.t.
O=N
H
N
O
O
O
61%

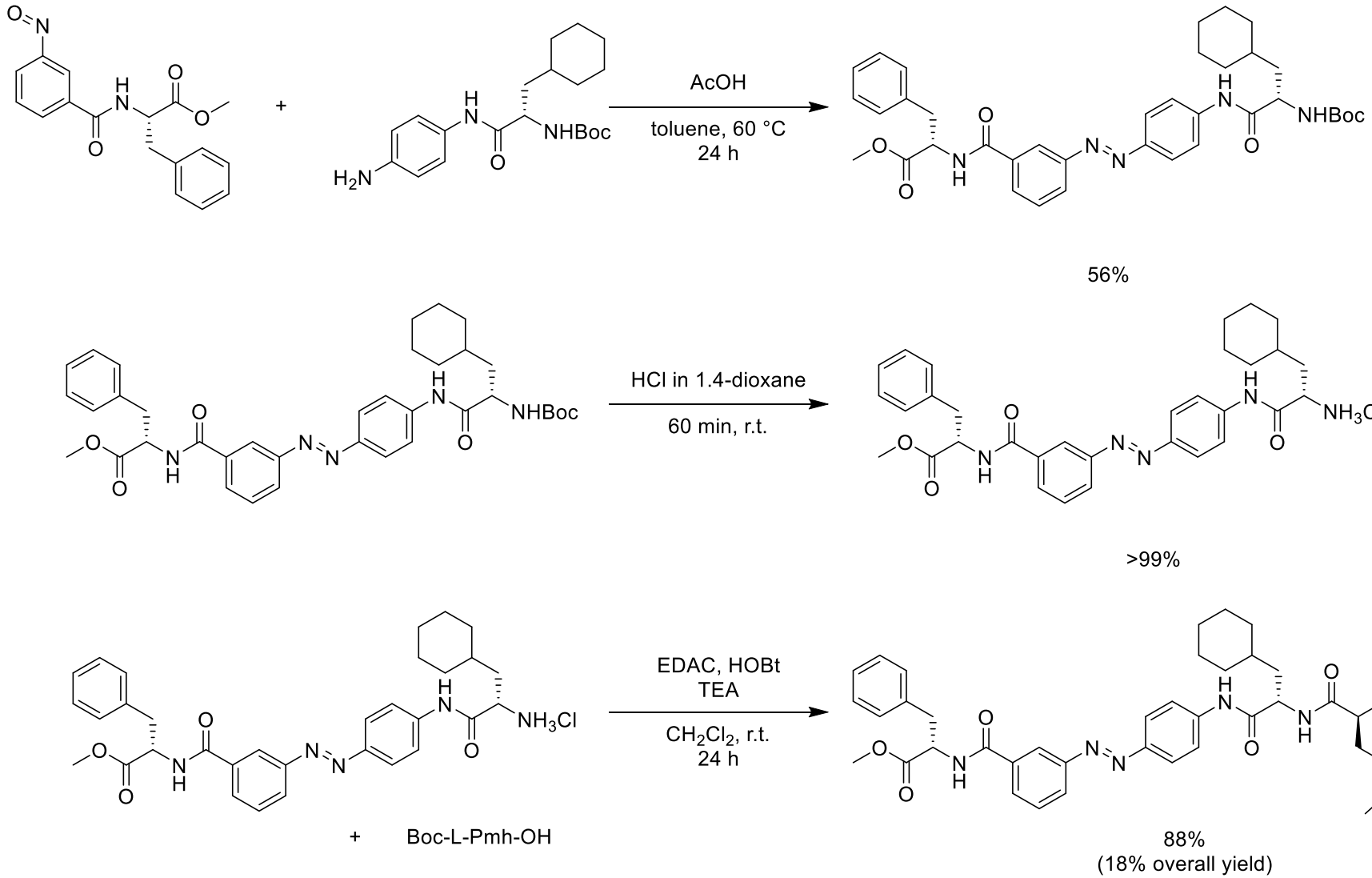
AcOH
toluene, 60 °C
24 h
56%
HCl in 1.4-dioxane
60 min, r.t.
>99%
EDAC, HOBt
TEA
CH2Cl2, r.t.
24 h
+ Boc-L-Pmh-OH
88%
(18% overall yield)

Synthesized Catalysts

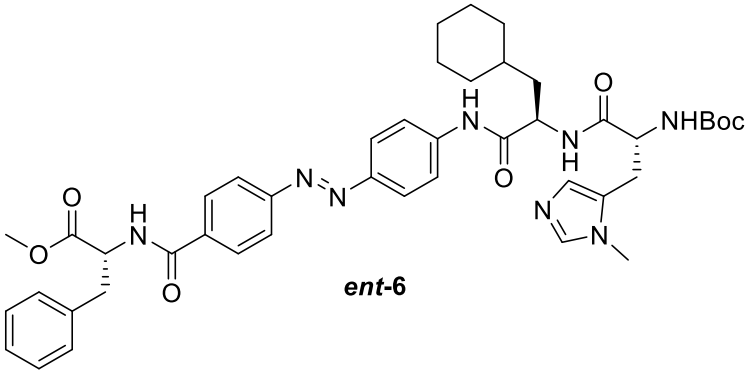

***ent*-6**

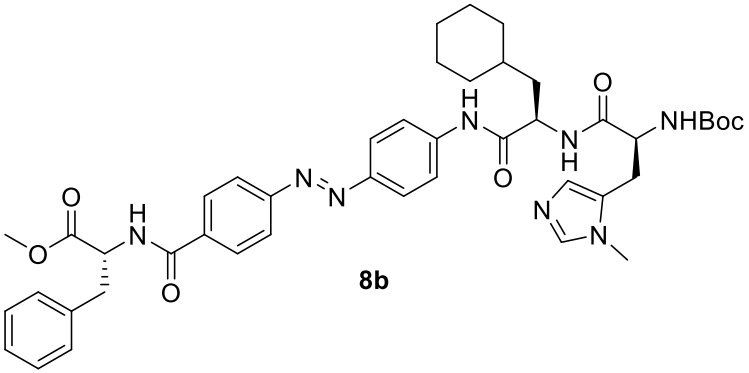

8b

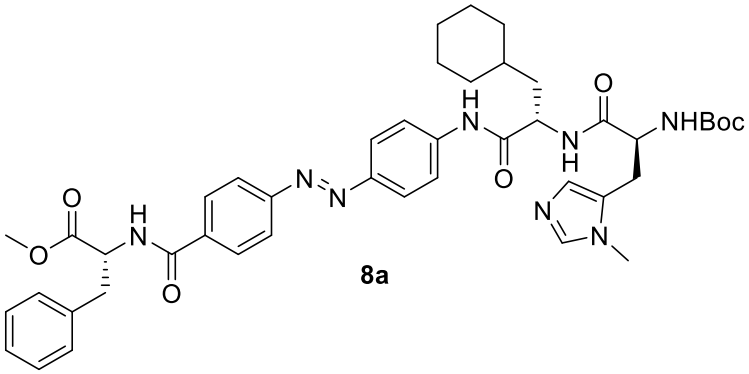

8a

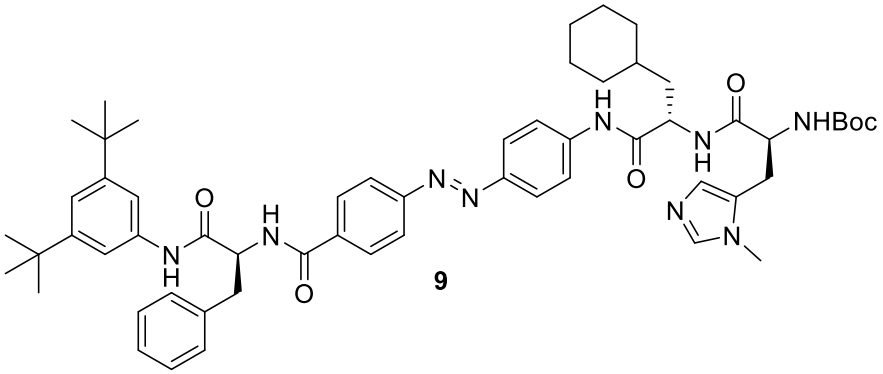

9

Acetylation of (4,6-*O*-benzylidene)methyl-α-D-glucopyranoside **1**

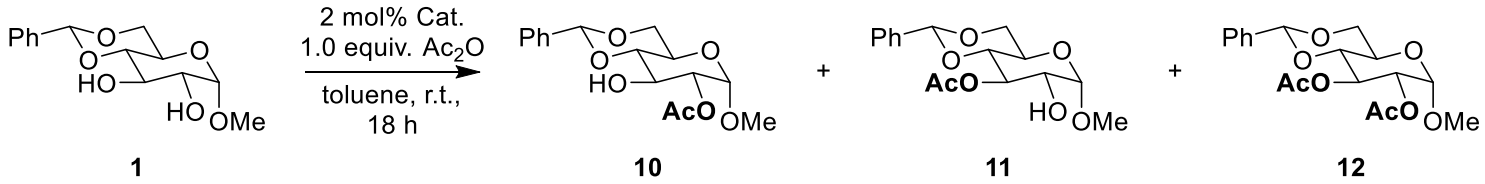

Catalyst	**10**[a]	**11**[a]	**12**[a]	Yield[a] / %
NMI	3.0	10.6	1.0	84
4	6.4	3.8	1.0	81
4 (365 nm)	4.8	2.6	1.0	90
5	17.3	6.8	1.0	62
5 (365 nm)	5.5	3.5	1.0	83
6[b]	9.4	7.1	1.0	88
6 (365 nm)	8.8	9.4	1.0	80

[a] Yield and ratio determined *via* ^{1}H NMR. [b] Reaction at 0 °C. NMI = *N*-methylimidazol.

Acetylation of (4,6-*O*-benzylidene)methyl-α-D-galactopyranoside **2**

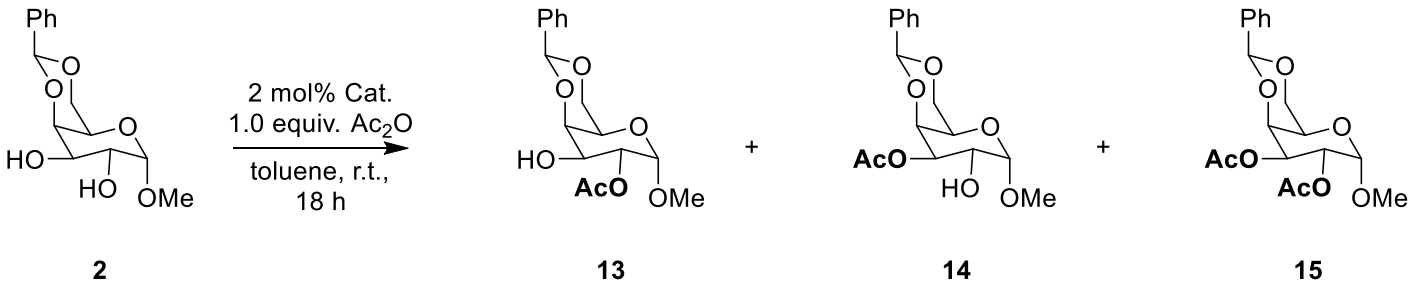

Catalyst	**13**[a]	**14**[a]	**15**[a]	Yield / %[b]
NMI	4.8	6.6	1.0	14
5	8.3	30.1	1.0	48
5 (365 nm)	11.1	18.0	1.0	75
6	2.8	9.7	1.0	79
6 (365 nm)	6.3	9.4	1.0	81
6 (365 nm)[c]	7.0	7.6	1.0	77

[a] Ratio was determined *via* NMR. [b] Yield was determined *via* NMR. [c] Reaction was carried out at 0°C.

Acetylation of (4,6-*O*-benzylidene)methyl-α-D-mannopyranoside **3a**

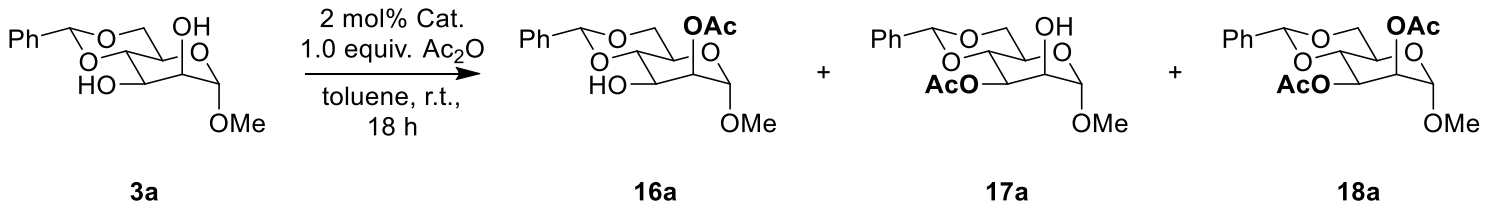

3a **16a** **17a** **18a**

Catalyst	**16a**[a]	**17a**[a]	**18a**[a]	Yield / %[a]
NMI	1.1	8.1	1.0	44
6	2.3	1.1	1.0	62
6 (448 nm)[b]	1.8	1.0	1.0	66
6 (365 nm)	1.0	4.7	3.4	61
6 (365 nm)[c]	1.0	7.4	3.2	66
6 (365 nm)[b, c]	1.0	19.8	10.1	74
7	1.7	1.0	1.1	68
7 (365 nm)[c]	1.0	11.9	7.0	77

[a] Yield and ratio determined *via* ^{1}H NMR. [b] 10 min irradiation before adding Ac_2O; reaction in the dark. [c] Reaction at 0 °C.

Acetylation of (4,6-*O*-benzylidene)methyl-α-D-mannopyranoside **3a-d**

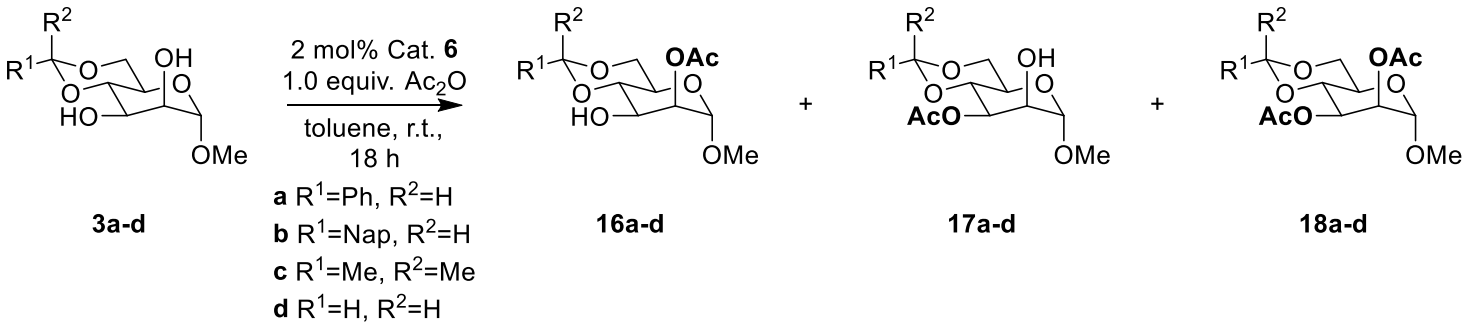

Substrate	**16a-d**[a]	**17a-d**[a]	**18a-d**[a]	Yield / %[a]
3a	2.3	1.1	1.0	62
3a (365 nm)[b]	1.0	19.8	10.1	74
3b	2.0	1.0	2.2	42[d]
3b (365 nm)[b]	1.0	10.7	9.5	25[d]
3c	3.9	3.6	1.0	75
3c (365 nm)[b]	1.8	4.0	1.0	91
3d	4.1	1.7	1.0	44[c]
3d (365 nm)[b]	1.0	10.4	6.1	54[c]

[a] Yield and ratio determined *via* ^{1}H NMR. [b] Reaction at 0 °C. [c] Yield not determined exactly due to some decomposition of the methylidene protecting group. [d] Low conversion due to solubility issues.

Acetylation of diphenylmethylene ketal protected quercetin **19**

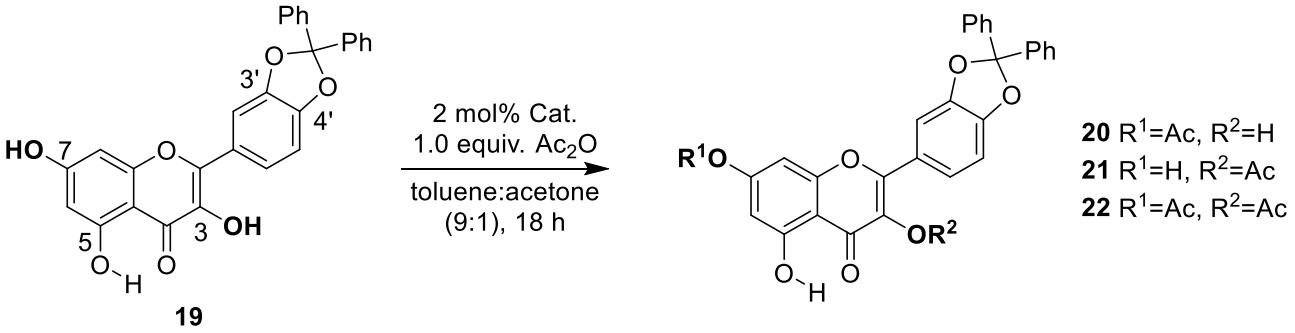

Catalyst	**20**[a]	**21**[a]	**22**[a]	Yield / %[a]
6	1.0	1.6	2.0	68
6 (365 nm)	1.3	1.0	1.5	73
6 (365 nm)[b]	5.0	1.0	4.0	86
6 (365 nm)[c]	7.7	1.0	6.1	80

[a] Yield and ratio determined *via* ^{1}H NMR [b] Acetone. [c] THF.

Homemade catalysis device

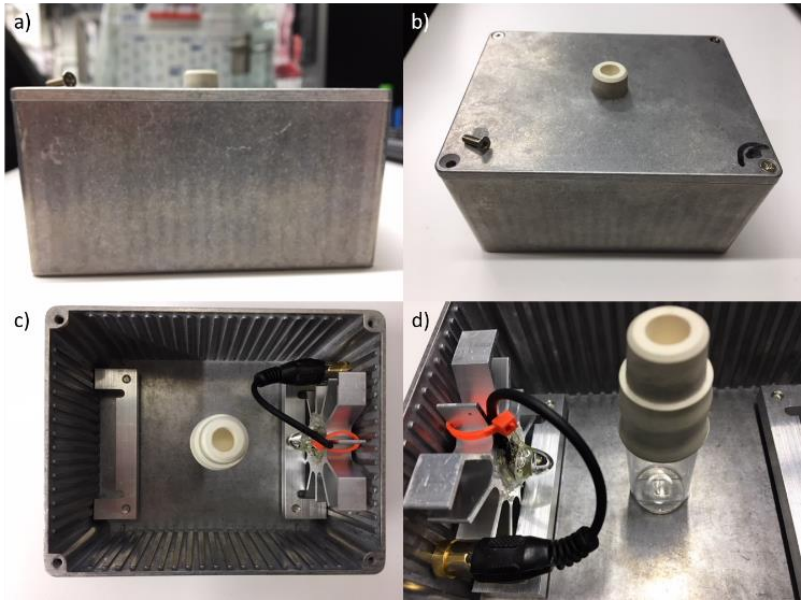

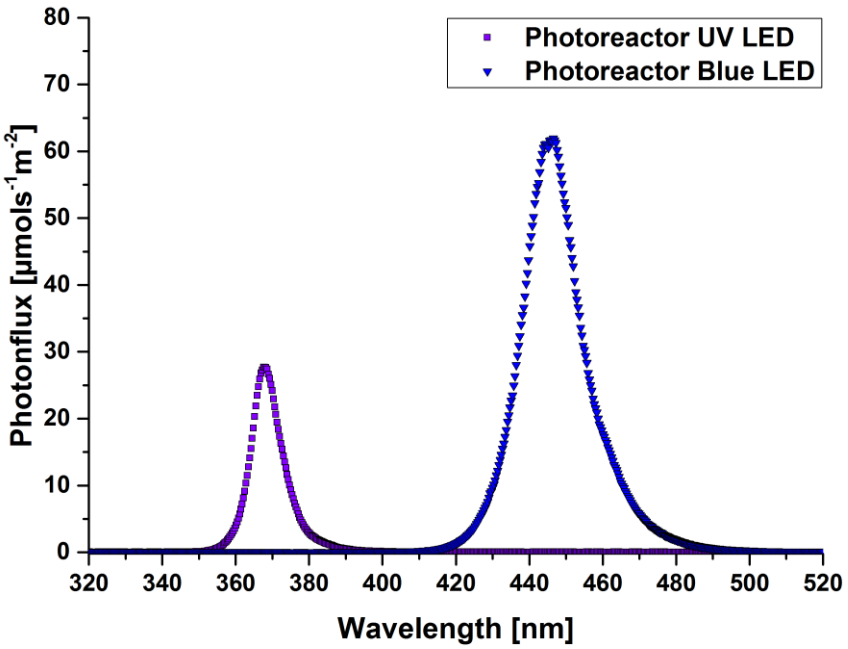

Homemade catalysis device; a) closed lightproof catalysis device b) reaction vessel equipped with septum to inject reactants and reagents c) inlet of the catalysis device with support for the LED and d) close-up view of the LED reaction vessel area: (right) Emission spectra of the UV LED (purple) and Blue LED (blue) used within the photoreactor.

Investigation of Catalyst 6 *via* ^{1}H and ^{13}C NMR spectroscopy

	E isomer		*Z* isomer	
Atom number	δ_H [ppm]	δ_C [ppm]	δ_H [ppm]	δ_C [ppm]
1	3.73	51.9	3.68	51.6
2	-	172	-	172
3	4.48	53.9	4.43	53.9
4	3.1-2.9	26.4	3.1-2.9	26.4
5	-	138.2	-	138.2
6	7.43	129.3	7.38	129.2
7	7.34	128.4	7.30	128.4
8	7.25	126.7	7.22	126.7
9	7.14	-	7.10	-
10	-	166.2	-	166.1
11	-	135.8	-	-[1]
12	8.16	128.9	7.92	128.5
13	7.99	122.5	7.01	119.7
14	-	154.1	-	-[1]
15	-	148.4	-	-[1]
16	8.02[2]	124	6.96	122.2
17	8.02[2]	119.7	7.67	119.1
18	-	143.3	-	-[1]
19	10.63	-	10.34	-
20	-	172.4	-	172
21	4.7	51.9	4.59	51.8
22	1.73	39.7	1.62	39.7
23-26	1.8 -0.8	39.8 – 26.1	-	-
27	8.42	-	8.40	-
28	-	-[1]	-	-[1]
29	4.87	54.9	4.78	54.9
30	3.3	36.5	3.2	36.5
31	-	-[1]	-	-[1]
32	6.81	127.6	6.79	127.6
33	7.56	137.9	7.54	137.9
34	3.65	137.9	3.65	137.9
35	9.2	-	9.02	-
36	-	166	-	166
37	-	79.8	.	79.8
38	1.38	27.9	1.34	27.9

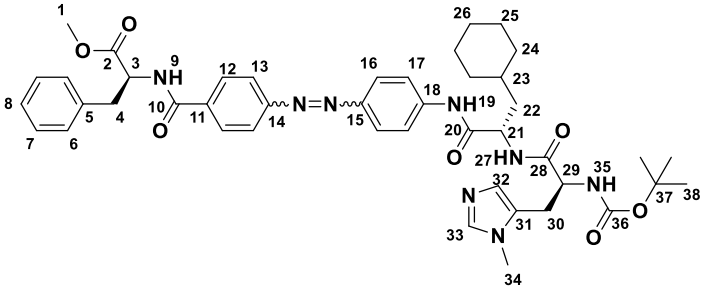

^{1}H and ^{13}C chemical shift assignment for the E and Z isomer of catalyst **6** in DMF-d_7 at 273 K.

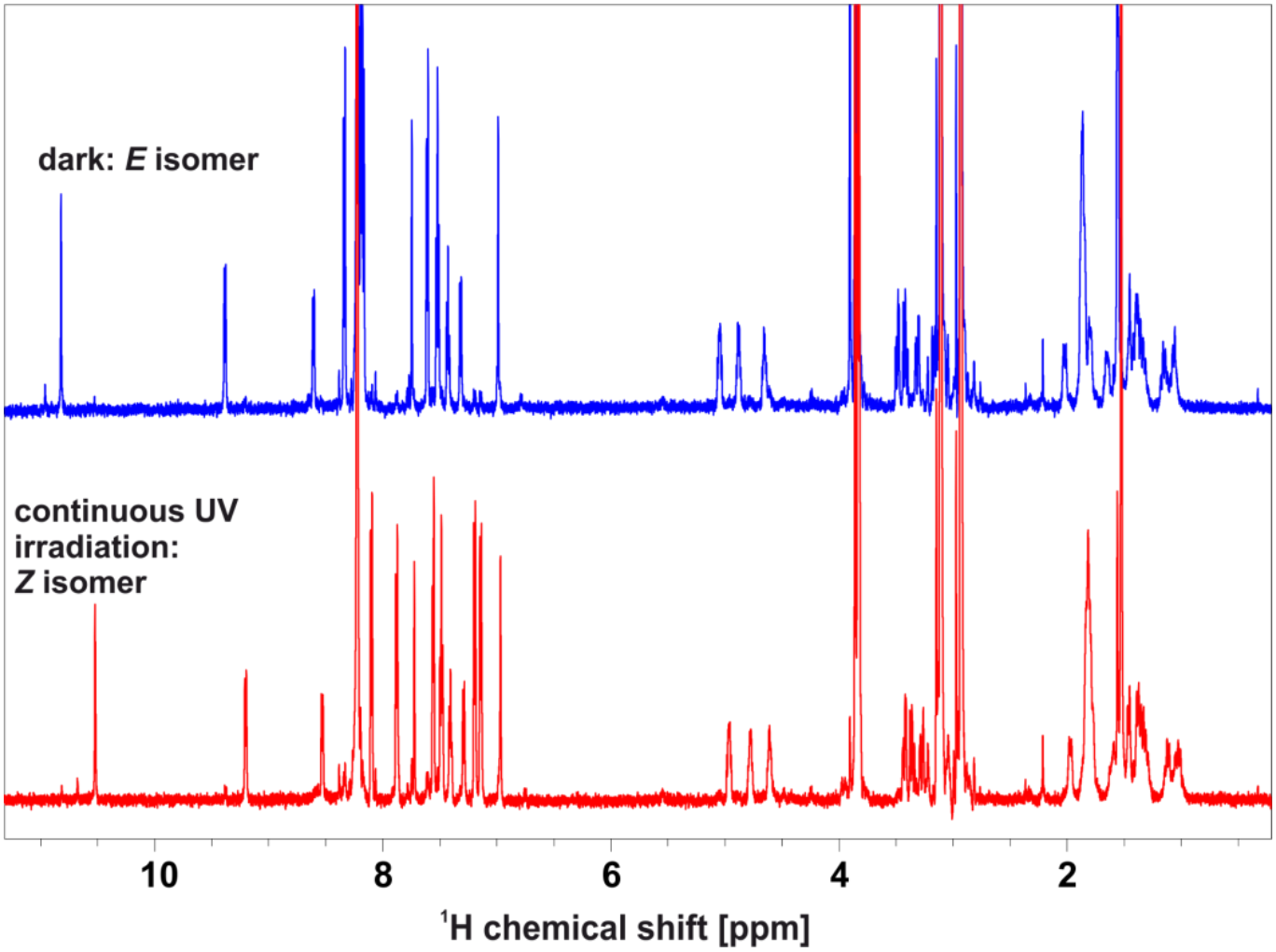

^{1}H NMR spectra (600 MHz proton resonance frequency) of a 1.3 mM solution of catalyst **6** in DMF-d_7 at 273 K prior to irradiation (upper trace) and during continuous irradiation (lower trace) with UV light (λ = 375 nm).

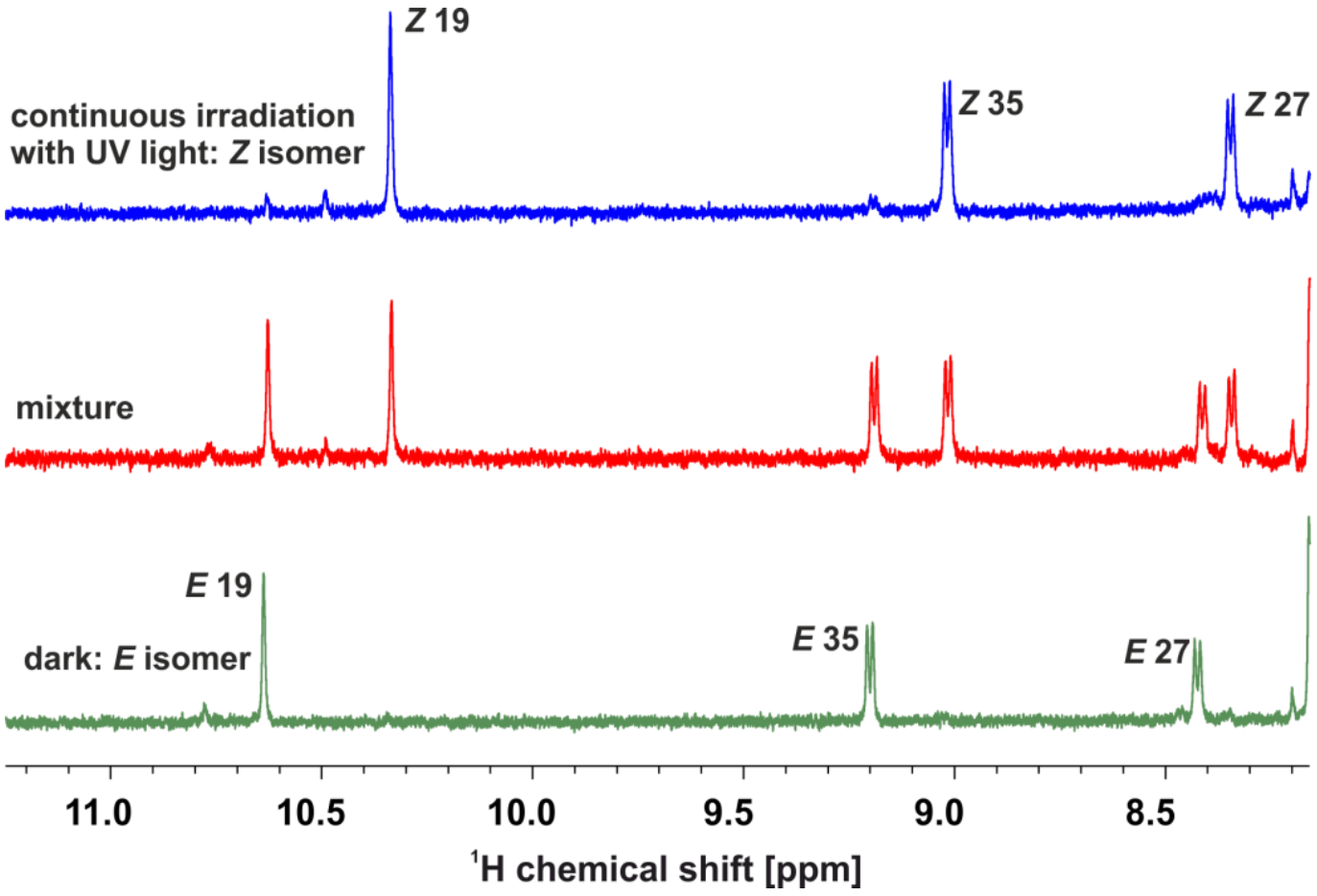

Amide signals in ^{1}H NMR spectra (600 MHz proton resonance frequency) of a 1.3 mM solution of catalyst **6** in DMF-d_7 at 273 K prior to irradiation (lower trace), of a mixture of E and Z isomer produced by an short irradiation interval and during continuous irradiation (upper trace) with UV light (λ = 375 nm).

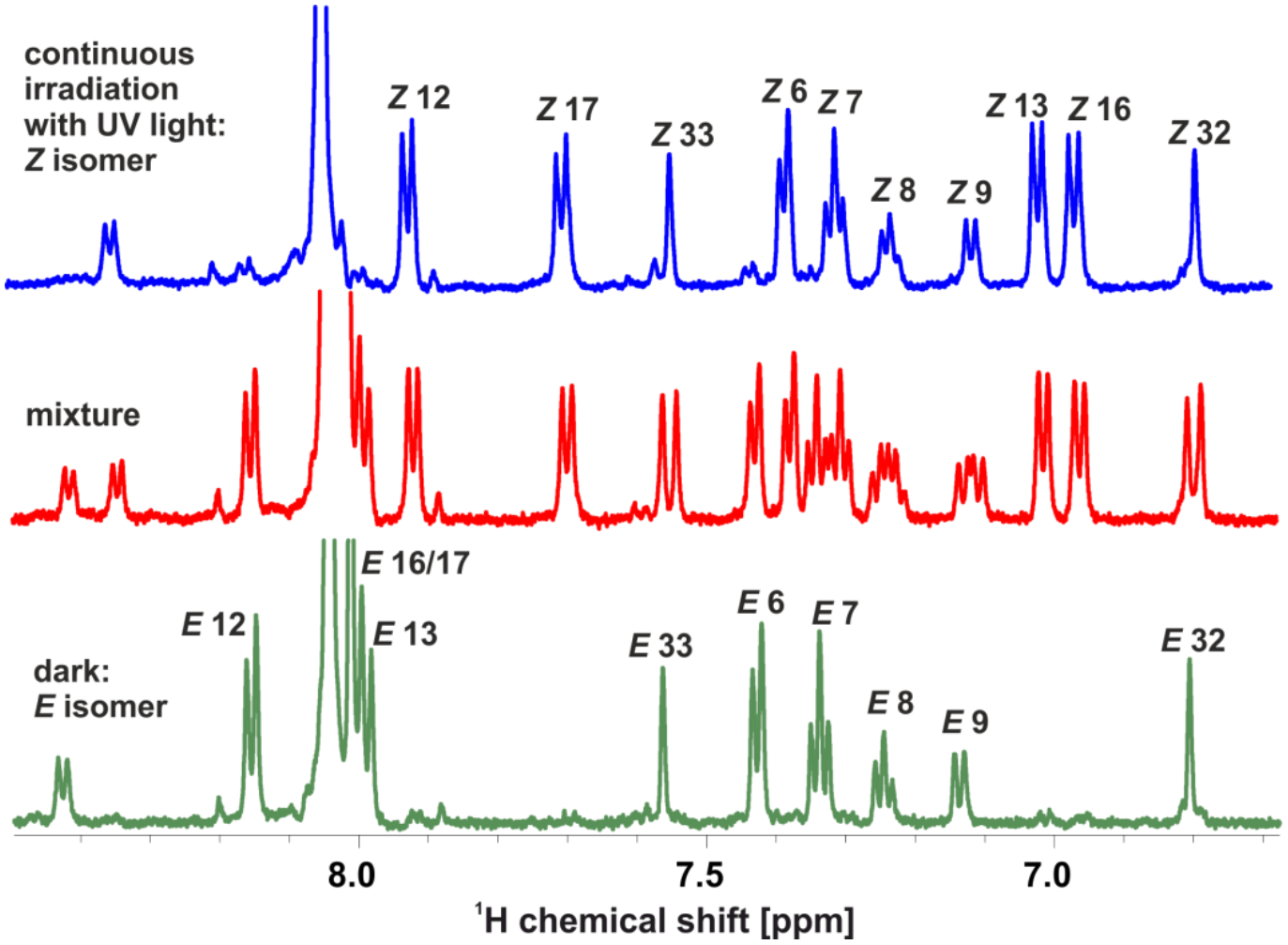

Aromatic resonances in ^{1}H NMR spectra of a 1.3 mM solution of catalyst **6** in DMF-d_7 at 273 K prior to irradiation (lower trace), of a mixture of E and Z isomer produced by an short irradiation interval and during continuous irradiation (upper trace) with UV light (λ = 375 nm).

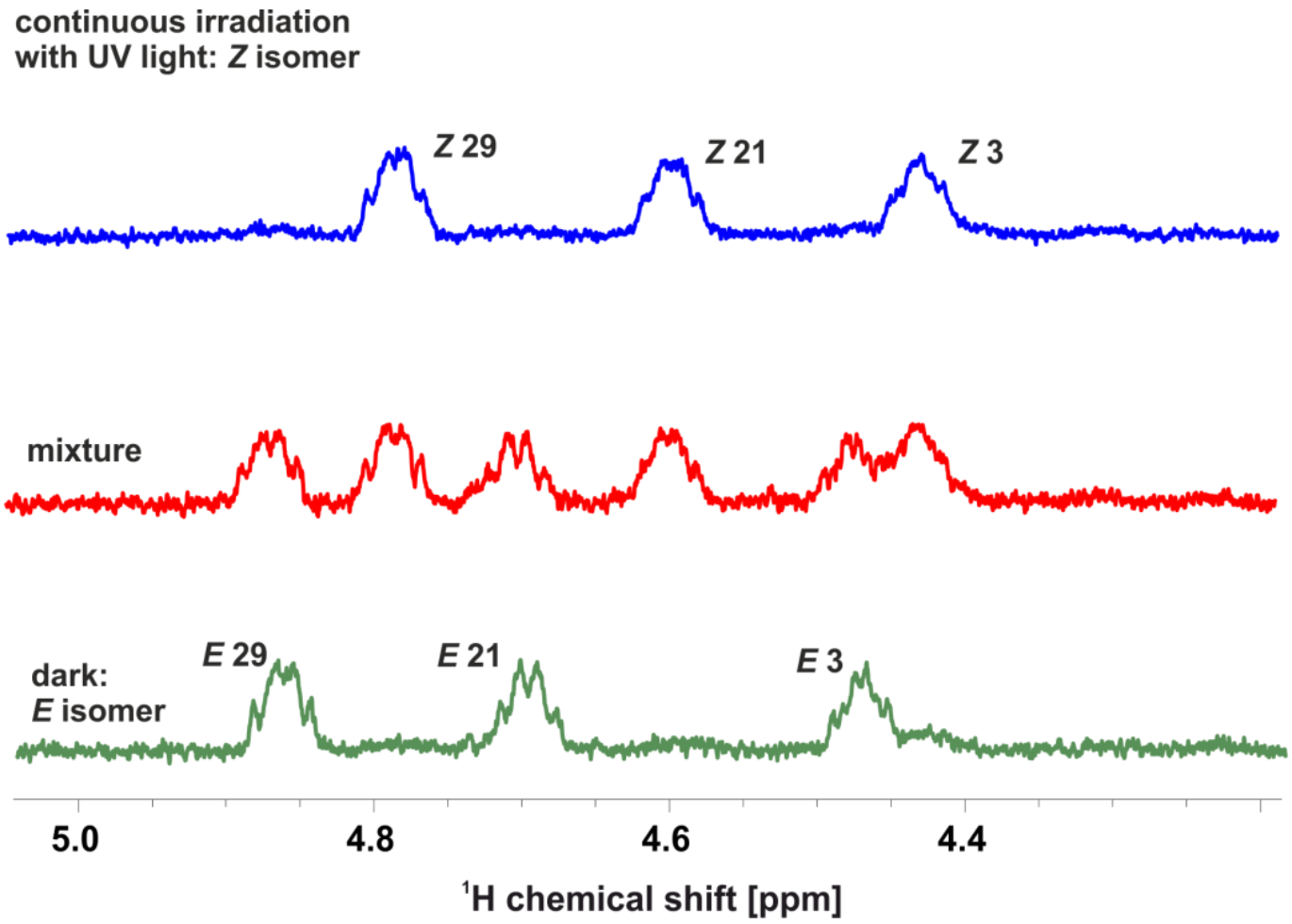

Resonances of protons in the α position of the peptide bonds in ^{1}H NMR spectra (600 MHz proton resonance frequency) of a 1.3 mM solution of catalyst **6** in DMF-d_7 at 273 K prior to irradiation (lower trace), of a mixture of E and Z isomer produced by an short irradiation interval and during continuous irradiation (upper trace) with UV light (λ = 375 nm).

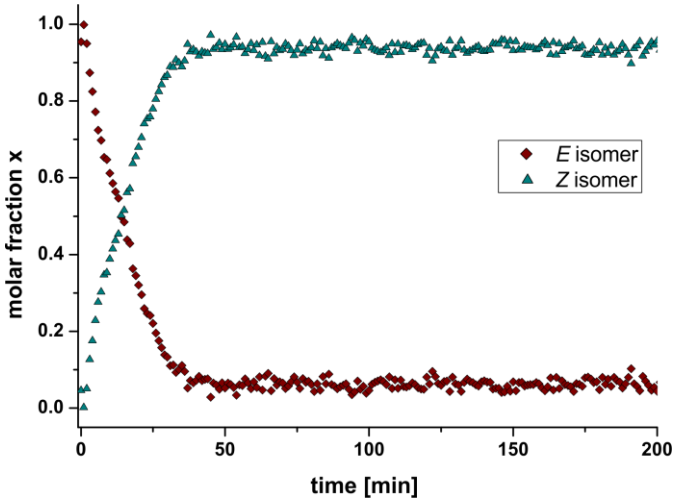

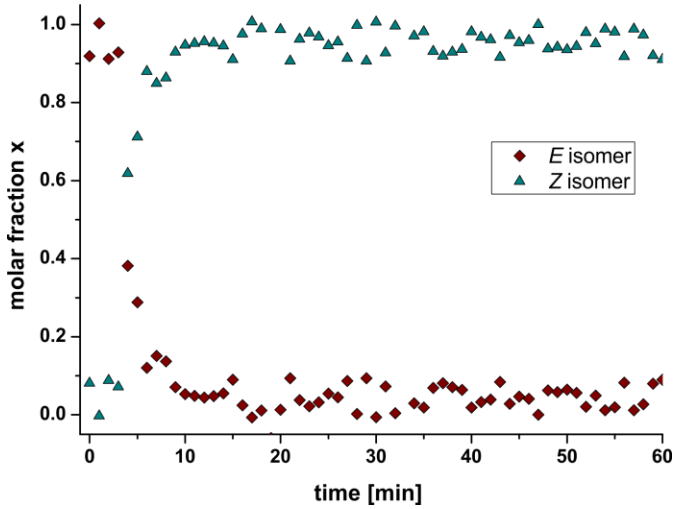

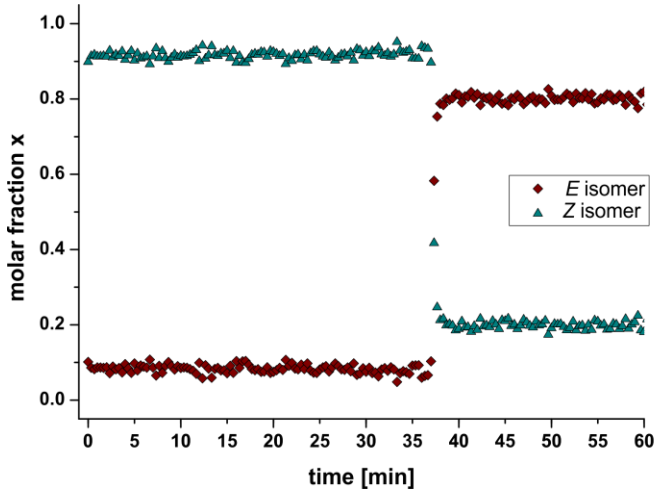

Molar fraction vs. time profiles for E (cyan) and Z (red) isomer of a 1.3 mM solution (left) and a 0.7 mM solution (right) of catalyst **6** in DMF-d_7 during continuous irradiation with UV light (λ = 375 nm) at 273 K. (top)

Molar fraction vs. time profiles for E (cyan) and Z (red) isomer of a 1.3 mM solution of catalyst **6** in DMF-d_6 during thermal fading after irradiation with UV light (λ = 375 nm) followed by continuous irradiation with blue light (λ = 448 nm) at 273 K. (bottom)

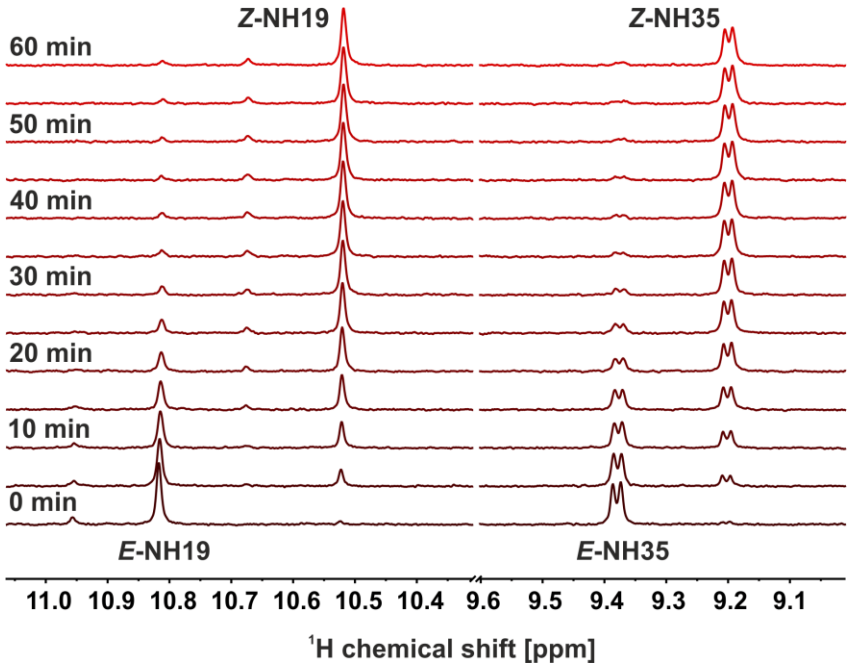

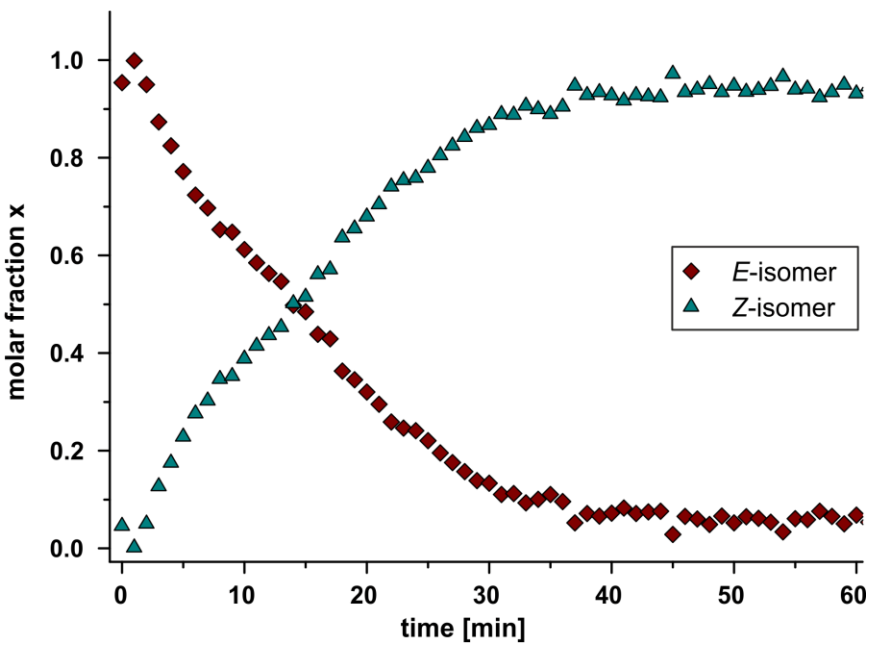

Kinetic profiles of the *E*→*Z* photoisomerization of catalyst 6. Left: stacked plot of ^{1}H NMR spectra in DMF-d_7 at 0 °C for the amide protons NH19 (located between the azo- and Pmh moieties) and NH35 (located at the Boc protecting group). Right: relative concentration profiles of the *E*- and *Z*-isomers with respect to the amide proton NH19 at the timescale of 1 hour.

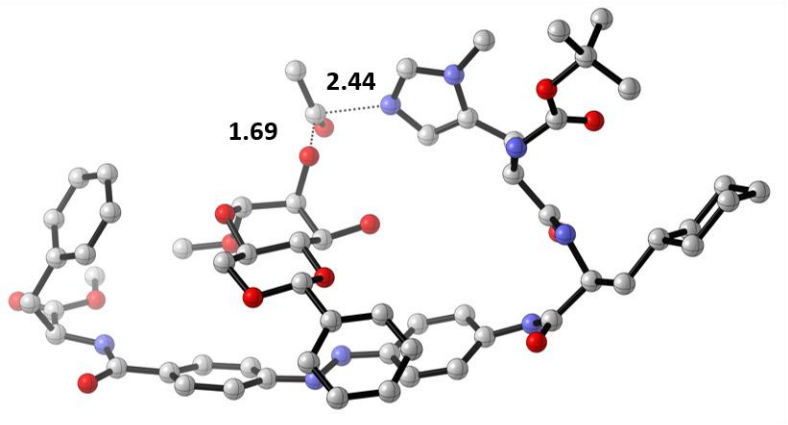

***E*-6‡**
inside catalytic event
(2-acetylation)

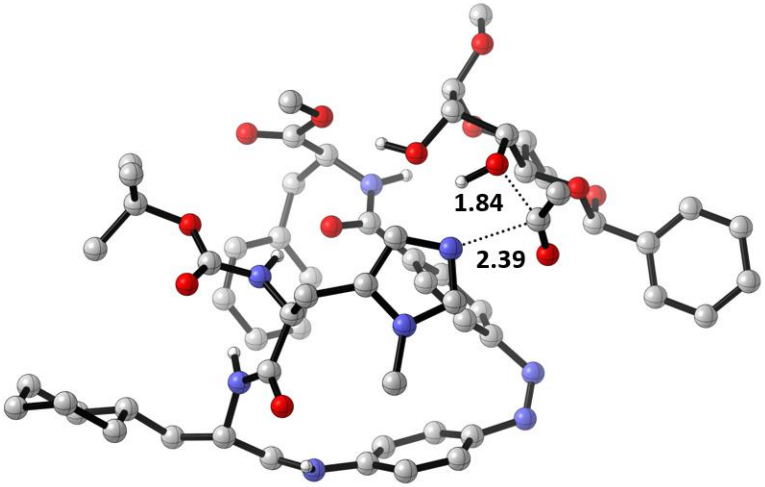

***Z*-6‡**
outside catalytic event
(3-acetylation)

Computed acetylation transition structures. Acetylation of (4,6-*O*-benzylidene)methyl-α-D-mannopyranoside **3a** at B3LYP-D3(BJ)/6-31G(d); transition state for the 2-acetylation resulting from ***E*-6** and **3a** (left) and transition state for the 3-acetylation resulting from ***Z*-6** and **3a** (right)

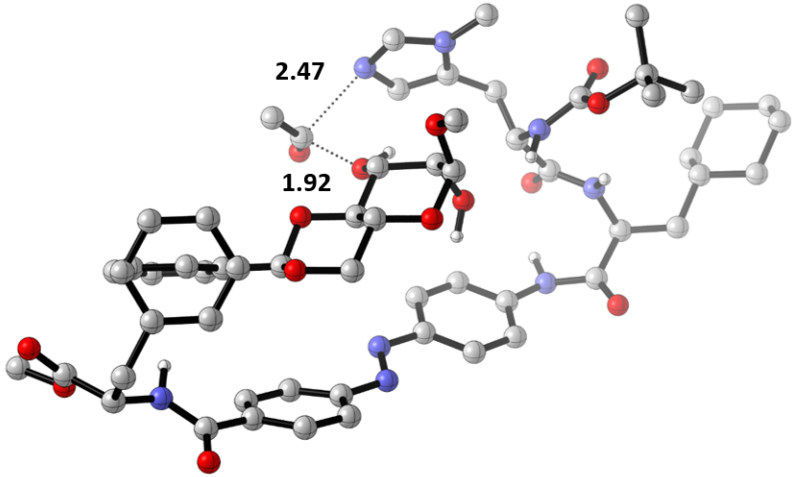

***E*-6‡**
inside catalytic event
(3-acetylation)

ΔE 3.8 (2.3) kcal mol^{-1}

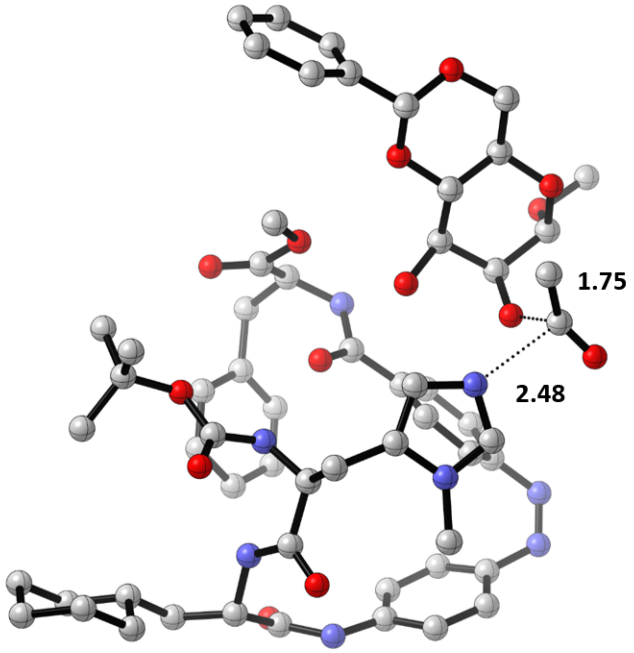

***Z*-6‡**
outside catalytic event
(2-acetylation)

ΔE 6.9 (6.0) kcal mol^{-1}

Computed acetylation transition structures. Acetylation of (4,6-*O*-benzylidene)methyl-α-D-mannopyranoside **3a** at B3LYP-D3(BJ)/6-31G(d) and B3LYP-D3(BJ)/cc-pVTZ//B3LYP-D3(BJ)/6-31G(d) (in parentheses); transition state for the 3-acetylation resulting from ***E*-6** and **3a** (left) and transition state for the 2-acetylation resulting from ***Z*-6** and **3a** (right)

Acknowledgment

- Prof. Dr. Peter R. Schreiner
- JPB, Eschi and Jan
- Alex, Raffi, Markus,Christopher and Freddy
- Dr. Heike Hausmann, Steffen Wagner, Stefan and Anika Bernhardt
- PRS-Group

Thank you for your attention!

http://launchany.com/wp-content/uploads/2016/01/idea.jpg